

In the above relations, C and D stand for the restoring force constant and the inertia of the vibrational mode, respectively.

$(C/D)^{1/2}$, the associated ZPF = $(\hbar^2/(2D\hbar\omega))^{1/2}$ leading to dynamical violations of rotational invariance. In the case in which $\langle Q_{2M} \rangle \neq 0$, the $|HF\rangle$ state is known as the Nilsson state, $|\text{Nilsson}\rangle$, defining a privileged orientation in 3D-space and thus an intrinsic, body-fixed system of reference \mathcal{K}' which makes an angle Ω (Euler angles) with the laboratory frame $\mathcal{K}^{(40)}$. Because there is no restoring force associated with the different orientations, fluctuations in Ω diverge in just the right way to restore rotational invariance, leading to a rotational band displaying a rigid moment of inertia (cf. Fig. 2.3.3 and 2.4.1), and whose members are the states⁽⁴¹⁾,

$$|IKM\rangle \sim \int d\Omega \mathcal{D}_{MK}^I(\Omega) |\text{Nilsson}(\Omega)\rangle; E_I = (\hbar^2/2I) I(I+1); I = I_{\text{rig}}.$$

One can also view such bands as the limit ($C \rightarrow 0, D (= I)$ finite) of low energy ($\omega \rightarrow 0$), large-amplitude collective vibration. Similar dynamic and static spontaneous symmetry breaking phenomena take place in connection with particle-particle ($\beta = +2$ transfer quantum number) and hole-hole ($\beta = -2$) correlations, namely in gauge space (see Fig. 2.4.1; subject discussed also in Sect. 2.5 (dynamic: pairing vibration) and also below (static: pairing rotation); see also Figs. 2.1.1, 2.1.3 and 2.1.4). For a consistent discussion of these subjects⁽⁴²⁾.

2.4.2 independent-pair motion

Let us make use of the constant pairing matrix element approximation $\langle j_1 j_2 | v | j_3 j_4 \rangle = G$, that is,

$$H_P = -G \sum_{\nu, \nu' > 0} a_\nu^\dagger a_\nu^\dagger a_{\nu'} a_{\nu'}. \quad (2.4.3)$$

The abnormal density is related to the finite value of the pair operator. The associated independent pair states are written in the BCS approximation as

$$(U_\nu^2 + V_\nu^2) = 1; \quad |\varphi_{\nu\bar{\nu}}\rangle = \left(U_j + V_j a_{jm}^\dagger a_{j\bar{m}}^\dagger \right) |0\rangle, \quad \begin{cases} V_\nu \\ U_\nu \end{cases} = \frac{1}{\sqrt{2}} \left(1 \mp \frac{\epsilon_\nu}{E_\nu} \right)^{1/2}, \quad (2.4.4)$$

where $E_\nu = \sqrt{\epsilon_\nu^2 + \Delta^2}$ and $\epsilon_\nu = \varepsilon_\nu - \lambda$, $\lambda = \varepsilon_F$. The BCS ground state,

$$|BCS\rangle = \prod_{\nu > 0} \left(U_j + V_j a_{jm}^\dagger a_{j\bar{m}}^\dagger \right) |0\rangle, \quad (2.4.5)$$

describes independent pair motion. Let us introduce the phasing⁽⁴³⁾,

$$U_\nu = |U_\nu| = U'_\nu; \quad V_\nu = e^{-2i\phi} V'_\nu; \quad (V'_\nu \equiv |V_\nu|) (\nu \equiv j, m), \quad (2.4.6)$$

⁽⁴⁰⁾Nilsson (1955).

⁽⁴¹⁾Bohr, A. and Mottelson (1975).

⁽⁴²⁾See Bès, D. R. and Kurchan (1990).

⁽⁴³⁾cf. e.g. Schrieffer, J. R. (1973).

namely a situation correctly described in term of strongly overlapping (quasibonic) pairs of fermion (Fig. 2.3.5), at variance with of that (erroneous) shown in Fig. 2.3.4).

where ϕ is the gauge angle. One can then write the (BCS) wavefunction as,

$$\begin{aligned} |BCS(\phi)\rangle_{\mathcal{K}} &= \prod_{\nu>0} (U'_{\nu} + V'_{\nu} e^{-2i\phi} a_{\nu}^{\dagger} a_{\bar{\nu}}^{\dagger}) |0\rangle = \prod_{\nu>0} (U'_{\nu} + V'_{\nu} a'_{\nu}^{\dagger} a'_{\bar{\nu}}^{\dagger}) |0\rangle \\ &= |BCS(\phi=0)\rangle_{\mathcal{K}'} : \text{lab. system, } \mathcal{K} : \text{intr. system } \mathcal{K}', \end{aligned} \quad (2.4.7)$$

where $a'_{\nu}^{\dagger} = e^{-i\phi} a_{\nu}^{\dagger}$ is the single-particle creation operator referred to the intrinsic system. The BCS order parameter, two-nucleon spectroscopic amplitudes and number and gap equations are, \star

$$\langle BCS | \sum_{\nu>0} a_{\nu}^{\dagger} a_{\bar{\nu}}^{\dagger} | BCS \rangle = \alpha'_0 e^{-2i\phi}; \quad \alpha'_0 = \sum_{\nu>0} U'_{\nu} V'_{\nu}; \quad \Delta = G \alpha'_0, \quad (2.4.8)$$

$$B_{\nu} = \langle BCS | [a'_{\nu}^{\dagger} a'_{\bar{\nu}}^{\dagger}]_0 | BCS \rangle = (j_{\nu} + 1/2)^{1/2} U'_{\nu} V'_{\nu}, \quad (2.4.9)$$

and

$$N_0 = 2 \sum_{\nu>0} V_{\nu}^2; \quad \frac{1}{G} = \sum_{\nu>0} \frac{1}{2E_{\nu}}. \quad (2.4.10)$$

Examples of B_{ν} -coefficients for the reaction $^{124}\text{Sn}(p, t)^{122}\text{Sn}(\text{gs})$ are given in Table 2.4.1.

The wavefunction and energies of the members of the pairing rotational band, can be written as

$$|N_0\rangle \sim \int_0^{2\pi} d\phi e^{-iN_0\phi} |BCS(\phi)\rangle_{\mathcal{K}} \sim \left(\sum_{\nu>0} c_{\nu} a_{\nu}^{\dagger} a_{\bar{\nu}}^{\dagger} \right)^{N_0/2} |0\rangle;$$

$$E_N = (\hbar^2/2I)N^2; \quad I \approx 2\hbar^2/G,$$

$$\hbar v_F / 2\Delta \approx 30 \text{ fm}$$

respectively⁴⁴.

In the case of a quadrupole deformed nucleus, the system acquires not only a privileged orientation in gauge space, but also in 3D-space. Now, as summarized above, in a superfluid system, Cooper pairs and not single-particles are the building blocks of the system (see Figs. 2.4.2 and 2.3.5)⁴⁵. But while the mean square radius of a nucleon at the Fermi energy ($\langle r^2 \rangle^{1/2} \approx (3/5)^{1/2} R_0$ ($R_0 = 1.2 A^{1/3} \text{ fm}$)) is about 4.6 fm ($A \approx 120$), that of a Cooper pair is determined by the correlation length ($\xi \approx \hbar v_F/m \approx 36 \text{ fm}$) between the two nucleons forming the pair (see Figs.

⁴⁴cf. e.g. Brink, D. and Broglia (2005) App. H; Mottelson (1998).

⁴⁵In connection with Fig. 2.4.2, the estimate $2R = 20/k_F$ was carried out with the help of the Fermi gas model (cf. e.g. Bohr and Mottelson (1969)). The Fermi momentum is written as $k_F \approx (3\pi^2 A/2V)^{1/3} \approx (\frac{3\pi^2}{2}\rho(0))^{1/3}$. Making use of $\rho(0) \approx 0.17 \text{ fm}^{-3}$ one obtains $k_F \approx 1.36 \text{ fm}^{-1}$.

Let us rewrite the relation between k_F and the volume $V (= (4\pi/3)R^3 = (4\pi/3)r_0^3 A)$. That is $k_F \approx (9\pi/8)^{1/3}/r_0 (= 1.52/r_0)$. Now, to employ $r_0 = 1.2 \text{ fm}$ and still keep 1.36 fm^{-1} , one has to modify the above relation to $k_F \approx 1.63/r_0$. Let us now write the diameter of a heavy nucleus of mass $A \approx 200$ ($A^{1/3} \approx 5.85$). i.e. $2R = 2r_0 A^{1/3} \approx 20/k_F$. This is the value used in Fig. 2.4.2.

We now

\star) See Potel et al (2017)

b) - d)

2.3.3 and 2.3.5). Consequently, orienting the quadrupole deformed potential in different directions (angles Ω), will have less effect on Cooper pairs than on independent particles. Thus the reduction of the moment of inertia from I_r to $\approx I_r/2$. Within this context one can mention the fact that low-lying nuclear collective vibrations (and rotations) are essentially not observed at intrinsic excitation energies corresponding to temperatures of $\approx 1\text{--}2$ MeV. In this case, this is because the surface is strongly fluctuating and thus not well defined, making it non operative its anisotropic orientation in space.

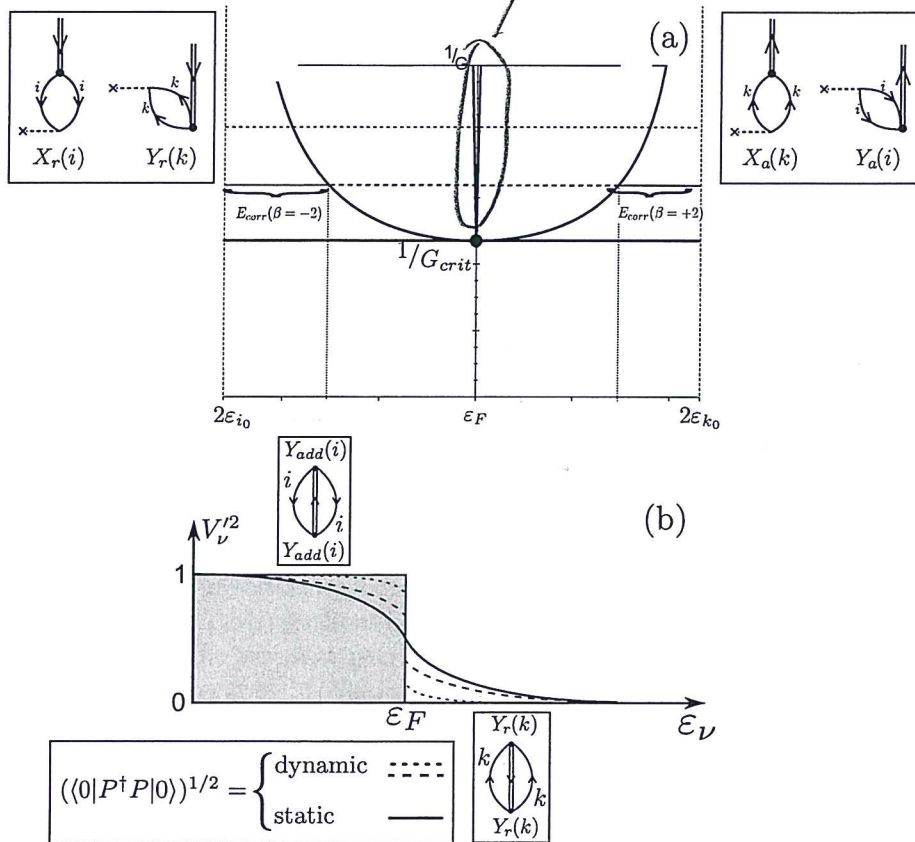
(thermally)

$nlj^a)$	$^{112}\text{Sn}(p, t)^{110}\text{Sn(gs)}$		$^{124}\text{Sn}(p, t)^{122}\text{Sn(gs)}$	
	BCS ^{b)}	$V_{low-k}^c)$	BCS ^{d)}	NuShell ^{e)}
$1g_{7/2}$	0.96	-1.1073	0.44	0.63
$2d_{5/2}$	0.66	-0.7556	0.35	0.60
$2d_{3/2}$	0.54	-0.4825	0.58	0.72
$3s_{1/2}$	0.45	-0.3663	0.36	0.52
$1h_{11/2}$	0.69	-0.6647	1.22	-1.24

Table 2.4.1: Two-nucleon transfer spectroscopic amplitudes associated with the reactions $^{112}\text{Sn}(p, t)^{110}\text{Sn(gs)}$ and $^{124}\text{Sn}(p, t)^{122}\text{Sn(gs)}$. a) quantum numbers of the two-particle configurations $(nlj)_{J=0}^2$ coupled to angular momentum $J = 0$. b),d) $\langle \text{BCS} | P_\nu | \text{BCS} \rangle = \sqrt{2j_\nu + 1} U_\nu(A) V_\nu(A+2)$ ($A+2 = 112$ and 124 respectively), where $P_\nu = a_\nu a_\nu$ ($\nu \equiv nlj$) (cf. Potel, G. et al. (2011, 2013a,b)) c) two-nucleon transfer spectroscopic amplitudes calculated making use of initial and final state wavefunctions obtained by diagonalizing a V_{low-k} , that is a renormalized, low-momentum interaction derived from the CD-Bonn nucleon-nucleon potential (see Guazzoni, P. et al. (2006) and references therein). e) Two-neutron overlap functions obtained making use of the shell-model wavefunctions for the ground state of ^{122}Sn and ^{124}Sn calculated with the code NuShell (Brown, B. A. and Rae, 2007). The wavefunctions were obtained starting with a G -matrix derived from the CD-Bonn nucleon-nucleon interaction Machleidt, R. et al. (1996). These amplitudes were used in the calculation of $^{124}\text{Sn}(p, t)^{122}\text{Sn}$ absolute cross sections carried out by I.J. Thompson (Thompson, I.J., 2013).

Because in FMBS quantal fluctuations are very important⁴⁶, deformation in such systems explicit themselves through rotational bands. In particular, superfluid nuclei display well defined pairing rotational bands, an example of such bands being provided by the ground states of the superfluid Sn-isotopes. In this case, the moment of inertia is directly related to the pairing interaction. Pairing rotational bands are specifically excited in two nucleon transfer reactions (cf. Figs. 2.1.3 and 2.1.4). A summary of the physics which is at the basis of independent single-particle and single-pair motion is given in Figs. 2.4.2 and 2.4.3.

⁴⁶see Bertsch and Broglia (2005) and references therein.



✓ Figure 2.5.6: Schematic representation of the quantal phase transition taking place as a function of the pairing coupling constant in a (model) closed shell nucleus. (a) dispersion relation associated with the RPA diagonalization of the Hamiltonian $H = H_{sp} + H_p$ for the pair addition and pair removal modes. In the insets are shown the two-particle transfer processes exciting these modes, which testify to the fact that the associated zero point fluctuations (ZPF) which diverge at $G = G_{crit}$, blur the distinction between occupied and empty states typical of closed shell nuclei. (b) occupation number associated with the single-particle levels. For $G < G_{crit}$ there is a dynamical depopulation (population) of levels $i(k)$ below (above) the Fermi energy. For $G > G_{crit}$, the deformation of the Fermi surface becomes static, although with a non-vanishing dynamic component (cf. Fig. 2.1.2).

case of quadrupole surface distortions in 3D space⁽⁵⁰⁾. These results underscore the major role pairing vibrations play in nuclei around closed shells, while those collected in Fig. 2.1.2 their importance in gauge invariance restoration in systems far away from closed shells.

2.6 Halo pair addition mode and pygmy: a new mechanism to break gauge invariance

Pairing is intimately connected with particle number violation and thus spontaneous breaking of gauge invariance, as testified by the order parameter $\langle BCS | P^\dagger | BCS \rangle = \alpha_0$. In the nuclear case and, at variance with condensed matter, dynamical breaking of gauge symmetry is similarly important to that associated with static distortions (e.g. pairing vibrations around closed shell nuclei, cf. Fig. 2.1.1; see also Fig. 2.4.2 and Fig. 2.5.7) The fact that the average single-particle field acts as an external potential (like e.g. a magnetic field in metallic superconductors) is one of the reasons of the existence of a critical value G_c of the pairing strength G to bind Cooper pairs in nuclei. Spatial quantization in finite systems at large and in nuclei in particular, is intimately connected with the paramount role the surface plays in these systems⁽⁵¹⁾. Another consequence of this role is the fact that in nuclei an important fraction (30-50%) of Cooper pair binding is due to the exchange of collective vibrations between the partners of the pair⁽⁵²⁾, the rest being associated with the bare NN -interaction in the 1S_0 channel (cf. Fig. 2.6.1) plus possible $3N$ corrections⁽⁵³⁾. Within this context we note that the results displayed in Fig. 2.1.2 provide one of the clearest quantitative examples of the central and ubiquitous role pairing vibrations play in nuclear pairing correlations.

The study of light exotic nuclei lying along the neutron drip line have revealed a novel aspect of the interplay between shell effects and induced pairing interaction. It has been found that there are situations in which spatial quantization screens, essentially completely, the bare nucleon-nucleon interaction. This happens in the case in which the nuclear valence orbitals are s, p -states at threshold⁽⁵⁴⁾. An example of situations of this type is provided by $N = 6$ (parity inversion; cf. Chapter 4 Section 4.2.2) isotones. In particular, by ^{11}Li , in which case the strongly renormalized $s_{1/2}$ and $p_{1/2}$ valence orbitals are a virtual and a resonant state lying at ≈ 0.2 and 0.5 MeV in the continuum, respectively. Let us elaborate on this point. The binding provided by a contact pairing interaction $V_\delta(|\mathbf{r} - \mathbf{r}'|)$ (δ -force) to a pair of

⁽⁵⁰⁾For details cf. Bès and Broglia (1977), Broglia, R.A. et al. (1968), Bès, D. R. et al. (1988), Shimizu, Y. R. et al. (1989), Shimizu, Y. R. (2013), Vaquero et al. (2013) and references therein.

(pairing)

(^{10}Li)

Barranco
et al (1987)

⁽⁵¹⁾cf. Broglia, R. A. (2002) and references therein.

⁽⁵²⁾cf. e.g. Barranco et al. (1999), Brink, D. and Broglia (2005), Saperstein and Baldo (2013), Avdeenkov and Kamerdzhiev (2013), Lombardo et al. (2013), and references therein; cf. also Bohr, A. and Mottelson (1975), p. 432.

⁽⁵³⁾cf. e.g. Lesinski et al. (2012), Pankratov et al. (2011), Hergert and Roth (2009).

⁽⁵⁴⁾Pairing anti-halo effect; Bennaceur, K. et al. (2000), Hamamoto and Mottelson (2003), Hamamoto, I. and Mottelson (2004).

the dipole mode. From systematics, the centroid of these vibrations is $\hbar\omega_{GDR} \approx 100 \text{ MeV}/R$, R being the nuclear radius⁵⁷. Thus, in the case of ^{11}Li , one expects the centroid of the Giant Dipole Resonance carrying $\approx 100\%$ of the energy weighted sum rule (EWSR) at $\hbar\omega_{GDR} \approx 100 \text{ MeV}/2.7 \approx 37 \text{ MeV}$. Now, such a high frequency mode can hardly be expected to give rise to anything, but polarization effects (see within this context Eqs. 3.A.12–3.A.15). On the other hand, there exists experimental evidence which testifies to the presence of a rather sharp dipole state with centroid at $\approx 1 \text{ MeV}$ and carrying $\approx 8\%$ of the EWSR⁵⁸. The existence of this “pigmy resonance” which can be viewed as a simple consequence of the existence of a low-lying particle-hole state associated with the transition $s_{1/2} \rightarrow p_{1/2}$ testifies, arguably, to the coexistence⁵⁹ of two states with rather different radii in the ground state. One, closely connected with the ^9Li core, ($\approx 2.5 \text{ fm}$), the second with the diffuse halo ($\approx 4.6 \text{ fm}$), namely displaying a large radial deformation, and thus able to induce a conspicuous inhomogeneous damping to the dipole mode.

Before proceeding, let us estimate the overlap O between the two “ground states”. Making use of a schematic expression for the single-particle radial wave-functions

$$\mathcal{R} = \sqrt{3/R_0^3} \Theta(r - R_0), \quad (2.6.2)$$

where

$$\Theta = 1 \quad (r \leq R_0); \quad 0 \quad (r > R_0),$$

leading to,

$$\int_0^\infty dr r^2 \mathcal{R}^2(r) = \frac{3}{R_0^3} \int_0^{R_0} dr^3 / 3 = 1, \quad (2.6.3)$$

one can work out the overlap O between the two halo neutrons and the core nucleons.

one is talking about dipole radiation. To describe the de-excitation process of hot nuclei requires the knowledge of the photon interactions with excited states. The common assumption, known as the Axel-Brink hypothesis, has been that each excited state of a nucleus carries a giant dipole resonance (GDR) on top of it, and that the properties of such resonances are unaffected by any excitation of the nucleus (Brink (1955 (unpublished), Lynn (1968) pag. 321, Axel (1962); cf. also Bertsch, G. F. and Broglia (1986) and Bortignon, P. F. et al. (1998))

⁵⁷cf. e.g. Bortignon, P. F. et al. (1998) and Bertsch and Broglia (2005).

⁵⁸Zinser, M. et al. (1997), T. Nakamura et al. (2006), Shimoura et al. (1995), Ieki et al. (1993), Saekett et al. (1993), Kanungo et al. (2015), Kobayashi et al. (1989).

⁵⁹Within this context one can mention similar situations concerning the coexistence of spherical and quadrupole deformed states (cf. e.g. Wimmer, K. et al. (2010), Federman and Talmi (1965), Federman and Talmi (1966), Dönuau et al. (1967) and refs. therein; cf. also Bohr and Mottelson (1963)), typically of nuclei with $N \approx Z$. The fact that the associated inhomogeneous damping on the GDR has modest consequences concerning dipole strength at low energies as compared with radial (isotropic) deformations in ^{11}Li is understood in terms of the (non-Newtonian) plasticity of the atomic nucleus regarding quadrupole deformations (low-lying collective 2^+ surface vibrations, fission, exotic decay (cf. Barranco, F. et al. (1988), Barranco et al. (1989), Bertsch et al. (1987))), and of the little compressibility displayed by the same system and connected with saturation properties.

Bertsch (1988)

(in the present case)

2.6. HALO PAIR ADDITION MODE AND PYGMY

155

That is,

$$\Theta = |\langle \mathcal{R}_{\text{halo}} | \mathcal{R}_{\text{core}} \rangle|^2 = \left(\sqrt{\frac{3}{R_0^3}} \sqrt{\frac{3}{R^3}} \int_0^\infty dr r^2 \Theta(r - R) \Theta(r - R_0) \right)^2 \\ = \left(\sqrt{\frac{3}{R_0^3}} \sqrt{\frac{3}{R^3}} \int_0^{R_0} dr^3 / 3 \right)^2 = (R_0/R)^3 = 0.16, \quad (2.6.4)$$

where use has been made of $\Theta(r - R)\Theta(r - R_0) = \Theta(r - R_0)$, $R_0 = 1.2A^{1/3}\text{fm} = 2.5\text{fm}(A = 9)$ and $R = (4.6 \pm 0.13) \text{ fm}$. Because of the small value of this overlap, one can posit that a *bona fide* dipole pigmy resonance is a GDR based on an exotic, unusually extended state as compared to systematics ($A \approx (4.6/1.2)^3 \approx 60$), i.e. to a system with an effective A mass number about 5 times that predicted by systematics.

Of notice that, the small values of r and of Θ have essentially the same origin. On the other hand, they have apparently rather different physical consequences. In fact, the first makes the bare interaction strength G subcritical, while the second one screens the repulsive symmetry potential $V_1 (\approx +25 \text{ MeV}, \text{cf. e.g. Bortignon, P. F. et al. (1998)})$, that is, the price one has to pay to separate protons from neutrons. This effect allows for a consistent fraction of the dipole Thomas-Reiche-Kuhn sum rule, that is of the $J^\pi = 1^-$ energy weighted sum rule (EWSR), to come low in energy from the value $E_{GDR} \approx (80/A^{1/3}) \text{ MeV}$ and, acting as an intermediate boson between the two halo neutrons, glue them to the ${}^9\text{Li}$ core. Summing up, the halo anti-pairing effect $G_{\text{screened}} = r \times G \ll G < G_{\text{crit}}$ triggers $(\Theta V_1 \ll V_1)$ the virtual presence of a "gas" of dipole (pigmy) bosons which, exchanged between the two halo neutrons (cf. Fig. 2.6.2), overcompensates the reduction of the bare pairing interaction, leading to the binding of the halo Cooper pair to the core (anti-halo anti-pairing effect). It can thus be stated that the halo of ${}^{11}\text{Li}$ and the pigmy resonance built on top of it constitute a pair of symbiotic states (see also Chapter 6, in particular Fig. 6.1.4).

Let us further elaborate on these issues. Making use of the relation $\langle r^2 \rangle^{1/2} \approx (3/5)^{1/2} R$ between mean square radius and radius, one may write

$$\langle r^2 \rangle_{{}^{11}\text{Li}} \approx \frac{3}{5} R_{\text{eff}}^2({}^{11}\text{Li}).$$

with

$$R_{\text{eff}}^2({}^{11}\text{Li}) = \left(\frac{9}{11} R_0^2({}^9\text{Li}) + \frac{2}{11} \left(\frac{\xi}{2} \right)^2 \right),$$

where

$$R_0({}^9\text{Li}) = 2.5\text{fm},$$

is the ${}^9\text{Li}$ radius ($R_0 = r_0 A^{1/3}$, $r_0 = 1.2\text{fm}$), while ξ is the correlation length of the Cooper pair neutron halo. An estimate of this quantity is provided by the relation

$$\xi = \frac{\hbar v_F}{2E_{\text{corr}}} \approx 20 \text{ fm},$$

in keeping with the fact that in ^{11}Li , $(v_F/c) \approx 0.1$ and $E_{corr} \approx 0.5$ MeV. Consequently,

$$R_{eff}(^{11}\text{Li}) \approx 4.83 \text{ fm} \quad (2.6.5)$$

and $\langle r^2 \rangle_{^{11}\text{Li}}^{1/2} \approx 3.74 \text{ fm}$, in overall agreement with the experimental value $\langle r^2 \rangle_{^{11}\text{Li}}^{1/2} = 3.55 \pm 0.1 \text{ fm}$ ⁶⁰. It is of notice that this value implies the radius $R(^{11}\text{Li}) = \sqrt{5/3 \langle r^2 \rangle_{^{11}\text{Li}}}$ ⁶¹ $\approx 4.58 \pm 0.13 \text{ fm}$.

We now proceed to the calculation of the centroid of the dipole pigmy resonance of ^{11}Li in the RPA making use of the separable interaction

$$H_D = -\kappa_1 \vec{D} \cdot \vec{D} \quad (2.6.6)$$

where $\vec{D} = \vec{r}$ and

$$\kappa_1 = \frac{-5V_1}{AR^2}. \quad (2.6.7)$$

The resulting dispersion relation is⁶¹

$$W(E) = \sum_{k,i} \frac{2(\epsilon_k - \epsilon_i) |\langle i | F | k \rangle|^2}{(\epsilon_k - \epsilon_i)^2 - E^2}. \quad (2.6.8)$$

Making use of this relation and of the fact that $\epsilon_{\nu_k} - \epsilon_{\nu_i} = \epsilon_{p_{1/2}} - \epsilon_{s_{1/2}} \approx 0.3 \text{ MeV}$, and that the EWSR associated with the ^{11}Li pigmy resonance is $\approx 8\%$ of the total Thomas–Reiche–Kuhn sum rule

$$\sum_n |\langle 0 | F | n \rangle|^2 (E_n - E_0) = \frac{\hbar^2}{2M} \int d\mathbf{r} |\vec{\nabla} F|^2 \rho(r), \quad (2.6.9)$$

which, for $F = r$ has the value $\hbar^2 A / 2M$ one can write⁶³,

$$2 \times 0.08 \times \frac{\hbar^2 A}{2M} = \frac{1}{\kappa_1} [(0.3 \text{ MeV})^2 - (\hbar \omega_{pigmy})^2],$$

and thus

$$(\hbar \omega_{pigmy})^2 = (0.3 \text{ MeV})^2 - 2 \times 0.08 \times \frac{\hbar^2 A}{2M} \kappa_1,$$

where⁶⁴

$$\kappa_1 = -\frac{5V_1}{A(\xi/2)^2} \left(\frac{2}{11} \right) = -\frac{125 \text{ MeV}}{A 100 \text{ fm}^2} \left(\frac{2}{11} \right) \approx \kappa_1^0 \times 0.045 = -\frac{2.5}{A^2} \text{ fm}^{-2} \text{ MeV},$$

⁶⁰Kobayashi, T. et al. (1989).

⁶¹cf. (3.30) p.55 of Bortignon, P. F. et al. (1998).

⁶²See Fig. 2.6.3; see also p.264 Brink, D. and Broglia (2005).

⁶³cf. Bertsch and Broglia (2005) pag. 53.

⁶⁴see Bortignon, P. F. et al. (1998).

the ratio in parenthesis reflecting the fact that only 2 out of 11 nucleons, slosh back and forth in an extended configuration with little overlap with the other nucleons, while

$$\kappa_1^0 = -\frac{5V_1}{AR_{eff}^2(^{11}\text{Li})} \approx 0.49 \text{ MeV fm}^{-2} \quad (2.6.10)$$

is the standard self consistent dipole strength⁶⁵. One then obtains,

$$-2 \times 0.08 \frac{\hbar^2 A}{2M} \kappa_1 = 2 \times 0.08 \times 20 \text{ MeV fm}^2 \times A \times \frac{2.5}{A^2} \text{ fm}^{-2} \text{ MeV} \approx 0.73 \text{ MeV}^2 \approx (0.85 \text{ MeV})^2.$$

Consequently

$$\hbar\omega_{pigmy} = \sqrt{(0.3)^2 + (0.85)^2} \text{ MeV} \approx 1.0 \text{ MeV},$$

in overall agreement with the experimental findings⁶⁶. It is of notice that the centroid of the pigmy resonance calculated in the RPA with the help of a separable dipole interaction is⁶⁷ $\approx (0.6 \text{ MeV} + 1.6 \text{ MeV})/2 \approx 1.0 \text{ MeV}$.

Let us now estimate the binding energy which the exchange of the pigmy resonance between two neutron of the Cooper pair halo of ¹¹Li can provide. The associated particle-vibration coupling⁶⁸ is $\Lambda = (\partial W(E)/\partial E|_{\hbar\omega_{pigmy}})^{-1/2}$. Note the use in what follows of a dimensionless dipole single-particle field $F' = F/R_{eff}(^{11}\text{Li})$. This is in keeping with the fact that one wants to obtain a quantity with energy dimensions ($[\Lambda] = \text{MeV}$), and that κ_1 has been introduced through the Hamiltonian H_D with the self consistent value normalized in terms of $R_{eff}^2(^{11}\text{Li})$. One then obtains

$$\begin{aligned} \Lambda^2 &= \left\{ 2\hbar\omega_{pigmy} \frac{2 \times 0.08(\frac{\hbar^2 A}{2M})/R_{eff}^2(^{11}\text{Li})}{[(\epsilon_{p_{1/2}} - \epsilon_{s_{1/2}})^2 - (\hbar\omega_{pigmy})^2]^2} \right\}^{-1}, \\ &= \left\{ 2 \text{ MeV} \frac{0.16(\hbar^2 A/2M)(1/4.83^2 \text{ fm}^2)}{[(0.3)^2 - (1 \text{ MeV})^2]^2 \text{ MeV}^4} \right\}^{-1}, \\ &= \left(\frac{3 \text{ MeV}^2}{(0.91)^2 \text{ MeV}^4} \right)^{-1}, \\ &= \left(\frac{1}{1.7} \right)^2 \text{ MeV}^2 \approx 0.35 \text{ MeV}^2, \end{aligned}$$

(Fig. 2.6.2)

leading to $\Lambda \approx 0.6 \text{ MeV}$. The value of the induced interaction matrix elements is then given by,

$$M_{ind} = \frac{2\Lambda^2}{DEN} = -\frac{2\Lambda^2}{\hbar\omega_{pigmy}} \approx -0.7 \text{ MeV}, \quad (2.6.11)$$

⁶⁵cf. Bohr, A. and Mottelson (1975).

⁶⁶Zinser, M. et al. (1997).

⁶⁷Barranco, F. et al. (2001); see also Fig. 11.3(a) p.269, Brink, D. and Broglia (2005).

⁶⁸cf. e.g. Brink, D. and Broglia (2005) Eq. (8.42) p.189.

Note

2.6. HALO PAIR ADDITION MODE AND PYGMY

**) That new physics, namely a novel mechanism to (dynamically) violate gauge invariance, finds a scenario of a barely bound Cooper pair at the drip line (half life 25 ms) to express itself seems to confirm a recurrent expectation¹⁵⁹ that truly new complex phenomena appear at the border between rigid order and randomness (see de Gennes (1994)).

Figure 2.6.2: Diagrammatic representation of the exchange of a collective 1^- pygmy resonance between pairs of nucleons moving in the time-reversal configurations $s_{1/2}^2(0)$ and $p_{1/2}^2(0)$. It is of notice that both these configurations can act as initial states the figure showing only one of the two possibilities. Consequently, the energy denominator to be used in the simple estimate (2.6.11) is the average value $DEN = (DEN_1 + DEN_2)/2 = -\hbar\omega_{\text{pigmy}}$ where $DEN_1 = \Delta\epsilon - \hbar\omega_{\text{pigmy}}$ and $DEN_2 = -\Delta\epsilon - \hbar\omega_{\text{pigmy}}$, while $\Delta\epsilon = \epsilon_{s_{1/2}} - \epsilon_{p_{1/2}}$.

the factor of two resulting from the two time ordering contributions (see Fig. 2.6.2). The resulting correlation energy is thus $E_{\text{corr}} = |2\epsilon_{s_{1/2}} - G' + M_{\text{ind}}| = |0.4 - 0.1 - 0.7| \approx 0.4$ MeV, in overall agreement with the experimental⁶⁹ findings (0.380 MeV). Of notice that in this estimate the (subcritical) effect of the screened bare pairing interaction has also been used (see Eq. (2.6.1)). **)

This schematic model has been implemented with microscopic detail⁷⁰ within the framework of a field theoretical description of the interweaving of collective vibrations and single-particle motion⁷¹, and is discussed in more detail within the context of single-particle (Chapter 4) and two-particle (Chapter 6) transfer processes. Here we provide a summary of the theoretical findings.

In Fig. 2.6.3 (I), the single-particle neutron resonances in ^{10}Li are given. The position of the levels $s_{1/2}$ and $p_{1/2}$ determined making use of mean-field theory is shown (hatched area and thin horizontal line, respectively). The coupling of a single-neutron (upward pointing arrowed line) to a vibration (wavy line) calculated making use of NFT Feynman diagrams (schematically depicted also in terms of either solid dots (neutron) or open circles (neutron hole) moving in a single-particle level around or in the ^9Li core (hatched area)), leads to conspicuous shifts in the energy centroid of the $s_{1/2}$ and $p_{1/2}$ resonances (shown by thick horizontal lines) and eventually to an inversion in their sequence. In Fig. 2.6.3 (II) the processes binding the halo neutron system ^{11}Li are displayed.

Starting with the clothed mean field picture in which two neutrons (solid dots) move in time-reversal states around the core ^9Li (hatched area) in the $s_{1/2}$ virtual state leading to an unbound $s_{1/2}^2(0)$ state where the two neutrons are coupled to angular momentum zero. The associated spatial structure of the uncorrelated pair is shown in a). The exchange of vibrations between the two neutrons displayed in the upper part of the figure leads to a density-dependent interaction which, added to

⁶⁹C. Bachelet et al. (2008), M. Smith et al. (2008).

⁷⁰cfr. Barranco, F. et al. (2001).

⁷¹Nuclear Field Theory (NFT); cf. Bortignon, P. F. et al. (1977) and references therein.

Barranco et al (2001)

*) see however Cavallaro et al (2017).

Bachelet et al PRL 100,

182501 (2008)

New binding energy for the two-neutron halo of ^{11}Li .

M. Smith et al PRL 101, 202501 (2008)

(add to
list of
refs.)

the nucleon-nucleon bare interaction (see boxed inset) which, as can be seen from the figure, is subcritical, correlates the two-neutron system leading to a bound state $|0\rangle$ whose wavefunction is displayed in b), together with the spatial structure of the Cooper pair. It is of notice that a large fraction of the induced interaction arises from the exchange of the pigmy resonance (see Fig. 2.6.2) between the two halo neutrons. Within this scenario one can posit that the ^{11}Li dipole pigmy resonance can hardly be viewed but in symbiosis with the ^9Li halo neutron pair addition mode and vice versa. For details see Chapter 6 as well as⁷².

Let us conclude this Section by stating that the detailed consequences of the diagonalization of self-energy processes and of the bare and induced interactions tantamount to the diagonalization of the many-body Hamiltonian, provides in the case of ^{10}Li an example of minimal mean field description (cf. apendice D de la introducción and App. 4.A) and, in the case of ^{11}Li , an example of the fact that pairs of dressed single-particle states lead to abnormal density (induced pairing interaction), also in the case of closed shell systems, due to the strong ZPF associated with pairing vibrations (Fig. 2.6.3, cf. (also discussion around Eq. (2.2.2)). In keeping with the fact that ^9Li is a normal, bound nucleus, while ^{10}Li is not bound testifies to the fact that the binding of two neutrons to the ^9Li core leading to ^{11}Li ground state ($S_{2n} \approx 380$ keV), is a pairing phenomenon.

Appendix 2.A Nuclear van der Waals Cooper pair

The atomic van der Waals (dispersive; retarded) interaction which, like gravitation, acts between all atoms and molecules, also non-polar, can be written for two systems placed at a distance R as (see App. 2.D),

$$\Delta E = -\frac{6 \times e^2 \times a_0^5}{R^6} = -\frac{6 \times e^2}{(R/a_0)^6} \frac{1}{a_0}, \quad (2.A.1)$$

where a_0 is the Bohr radius. A possible nuclear parallel can be established making the following correspondences,

$$e^2 \rightarrow \Lambda R_0 ({}^{11}\text{Li}) = 0.6 \text{ MeV} \times 2.7 \text{ fm}; \quad a_0 \rightarrow d = 4 \text{ fm}; \quad R \rightarrow R_{eff} ({}^{11}\text{Li}) = 4.83 \text{ fm}.$$

That is,

$$\begin{aligned} \Delta E &= -\frac{6 \times \Lambda \times R_0}{R^6} = -\frac{6 \times e^2}{(R_{eff} ({}^{11}\text{Li})/d)^6} \frac{1}{d} = \frac{6 \times 0.6 \text{ MeV} \times 2.7 \text{ fm}}{(4.83/4)^6} \frac{1}{4 \text{ fm}} \\ &= -\frac{9.72 \text{ MeV}}{12.4} \approx -0.8 \text{ MeV} \rightarrow M_{ind}. \end{aligned}$$

Thus,

$$E_{corr} = |2E_{s_{1/2}} - G' + \Delta E| = |0.4 \text{ MeV} - 0.1 \text{ MeV} - 0.8 \text{ MeV}| \approx 0.5$$

⁷²Barranco, F. et al. (2001).

~~write better~~
~~especially~~
 ~~$a_0 \rightarrow d = 4 \text{ fm}$~~

to be compared to

$$(S_{2n})_{exp} \approx 0.380 \text{ MeV.}$$

Appendix 2.B Renormalized coupling constants ^{11}Li : résumé

Let us make use of the experimental (empirical),

$$\epsilon_{s1/2} = 0.2 \text{ MeV},$$

$$\epsilon_{p1/2} = 0.5 \text{ MeV},$$

$$V_1 = 25 \text{ MeV},$$

and theoretical

$$R_0(^{11}\text{Li}) = 1.2(11)^{1/3} \text{ fm} = 2.7 \text{ fm},$$

$$\xi = 20 \text{ fm},$$

$$R_{eff}(^{11}\text{Li}) = 4.83 \text{ MeV},$$

$$G = \frac{25}{A} \text{ MeV} = 2.3 \text{ fm},$$

$$\kappa_1^0 = -\frac{5V_1}{A R_{eff}^{(11)\text{Li}}} \approx -0.49 \text{ MeV fm}^{-2},$$

$$\kappa_1 = -\frac{5V_1}{A(\xi/2)^2} = -0.021 \text{ MeV fm}^{-2},$$

i.e.

$$-\frac{5V_1}{A R_{eff}^{(11)\text{Li}}}$$

i.e.

$$K_1 = -\frac{5V_1}{A(\xi/2)^2} \left(\frac{2}{11}\right)$$

inputs.

One can then calculate the ratio

$$r = \frac{2}{(2j+1)} \frac{R_0}{R_{eff}}^3 \approx 0.042,$$

i.e.

$$-0.021$$

where use was made of $(2j+1) \approx (2k_F R_0 + 1) \approx 8.34$. Thus, the screened bare pairing interaction is,

$$(G)_{scr} = rG = 0.042 \times \frac{25}{A} \text{ MeV} = \frac{1 \text{ MeV}}{A} \approx 0.1 \text{ MeV.}$$

Similarly

$$\kappa_1 = s \kappa_1^0,$$

where the screening factor is

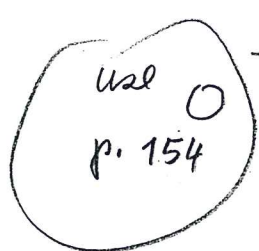
$$s = \frac{R_{eff}^2}{(\xi/2)^2} \frac{2}{11} \approx 0.042.$$

Thus, the screened symmetry potential is,

$$(V_1)_{scr} = sV_1 = 0.042 \times 25 \text{ MeV} = 1 \text{ MeV}.$$

The fact that r and s coincide within numerical approximations is in keeping with the fact that both quantities are closely related to the overlap

$$\mathcal{O} = \left(\frac{R_0}{R_{eff}} \right)^3 = \left(\frac{2.7 \text{ fm}}{4.83 \text{ fm}} \right)^3 = 0.17,$$



quantity which has a double hit effect concerning the mechanism which is at the basis of much of the nuclear structure of exotic nuclei at threshold: 1) it makes subcritical the screened bare NN -pairing interaction ($G)_{scr} = rG < G_c$ ($(G)_{scr} = 1 \text{ MeV/A}$); 2) it screens the symmetry potential drastically, reducing the price one has to pay to separate protons from delocalized neutrons, permitting a consistent chunk ($\approx 8\%$) of the TRK sum rule to become essentially degenerate with the ground state ($(V_1)_{scr} = 1 \text{ MeV}$), thus allowing for the first nuclear example of a van der Waals Cooper pair and a novel mechanism to break dynamically gauge invariance: dipole-dipole fluctuating fields associated with the exchange of the ^{dipole}pigmy resonance between the halo neutrons of ^{11}Li . As a result, a new, (composite) elementary mode of nuclear excitation joins the ranks of the previously known: the halo pair addition mode carrying on top of it, a low-lying collective pigmy resonance. This symbiotic mode can be studied through two-particle transfer reactions, eventually in coincidence with γ -decay. In particular, making use of the reactions,

$${}^9\text{Li}(t, p){}^{11}\text{Li}(f), \\ |f\rangle; \text{ ground state } (L = 0), \text{ pygmy } (L = 1),$$

and

$${}^{10}\text{Be}(t, p){}^{12}\text{Be}(f), \\ |f\rangle; \text{ first excited } 0^+ \text{ state } (E_x = 2.24 \text{ MeV}) (L = 0), \\ \text{pygmy on top of it } (L = 1, \text{ arguably the state at } E_x = 2.70 \text{ MeV is part of it}).$$

Appendix 2.C Lindemann criterion and connection with quantity parameter

Appendix 2.D The van der Waals interaction

*) Iwasaki et al (2000)

add to refs

H. Iwasaki et al. PLB 491, 8 (2000)